### International Journal of Analysis and Applications



# Steady-State Concentration and Current in Enhanced Modeling of Nonlinear Reaction-Diffusion Equations in Different Enzyme Kinetics

R. Vignesh Raju<sup>1</sup>, N. Jeeva<sup>2</sup>, Fady Hasan<sup>3</sup>, Nabil Mlaiki<sup>3</sup>, R. Swaminathan<sup>1,\*</sup>

<sup>1</sup>PG & Research Department of Mathematics, Vidhyaa Giri College of Arts and Science, Puduvayal 630108, Tamil Nadu, India

<sup>2</sup>Department of Mathematics, K.S.Rangasamy College of Technology, Tiruchengode 637215, Namakkal (Dt.), Tamil Nadu, India

<sup>3</sup>Department of Mathematics and Sciences, Prince Sultan University, Riyadh 11586, Saudi Arabia

\*Corresponding author: swaminathanmath@gmail.com

Abstract. The investigation of enzyme kinetics heavily relies on nonlinear reaction-diffusion equations to analyze biochemical reactions and intracellular diffusion processes. However, due to their inherent mathematical complexity, solving such equations presents significant challenges. Traditional analytical approaches often fail to yield exact solutions efficiently, necessitating the development of advanced and more effective modern techniques for obtaining accurate solutions. This study introduces an enhanced framework for modeling enzyme kinetics by employing the Akbari-Ganji Method (AGM) to address nonlinear reaction-diffusion equations. The proposed solution approach aims to achieve greater computational accuracy and efficiency. Owing to its inherent capabilities, the AGM effectively handles the nonlinear nature of reaction-diffusion systems. The validity of the developed method was confirmed through comparison with numerical simulations and established analytical techniques. This improved solution strategy provides deeper insights into enzyme kinetics, offering valuable applications in biochemical research and pharmaceutical development. Modern evaluation methods, such as AGM, overcome issues of computational complexity and limited precision, delivering faster and more reliable results than conventional techniques. Moreover, the AGM proves to be a robust and efficient tool for solving nonlinear reaction-diffusion equations relevant to enzyme kinetics and drug discovery processes.

#### 1. Introduction

Biosensors have found significant applications in diagnostic and industrial fields, particularly where real-time monitoring of biological systems is essential. However, enhancing their per-

Received: Apr. 24, 2025.

2020 Mathematics Subject Classification. 34A34, 34E10, 65L06.

*Key words and phrases.* Biosensor, Mathematical Modeling, Nonlinear Reaction Diffusion Equations, Enzyme Kinetics, Akbari-Ganji Method.

ISSN: 2291-8639

formance remains a major challenge due to the intricate interplay between enzyme kinetics and diffusion dynamics, which must be carefully balanced. These factors critically influence the efficiency, sensitivity, and reliability of biosensor systems. The underlying mechanisms of biosensor operation are governed by catalytic reactions and enzyme-substrate interactions, typically described by First-Order, Michaelis-Menten, and Ping-Pong kinetic models. Furthermore, diffusion phenomena arise from the movement of substrates and products, forming the fundamental basis of biosensor functionality. Modifying or extending these classical models often requires the application of advanced numerical methods, as analytical solutions are rarely feasible for complex, parameter-dependent systems.

To address the challenge of accurately characterizing performance variations caused by fluctuating reaction rates and substrate concentrations, Senthamarai et al. [3] investigated biosensor responses under non-steady-state substrate conditions for mixed enzyme kinetics. Joy Salomi et al. [5] explored transient responses in amperometric biosensors-particularly within phenolpolyphenol oxidase systems-providing valuable insights into the kinetic parameters influencing biosensor sensitivity and efficiency. A. Reena et al. [20] conducted a mathematical modeling study on urea-based amperometric biosensors under non-competitive inhibition, examining the influence of inhibitors on biosensor performance. Extending beyond conventional Michaelis-Menten kinetics, K. Nirmala et al. [7] analyzed steady-state substrate and product concentrations for biosensors incorporating complex kinetic behaviors such as allosteric modulation and cooperative binding, which are critical in practical biosensor applications. R. Usha Rani et al. [8] emphasized the role of product inhibition in amperometric biosensors and discussed potential strategies to mitigate its effects. Several researchers, including Swaminathan et al. [9], examined substrate inhibition phenomena, optimizing substrate concentrations and operating conditions to achieve improved sensitivity and optimal response. Hashem Zadeh et al. [10] investigated the influence of introducing holes in the membrane layer on analyte transport and reaction kinetics, proposing design strategies to enhance biosensor performance and responsiveness.

Sylvia et al. [11] advanced earlier biosensor models by incorporating nonlinear enzyme kinetics to describe amperometric biosensor behavior through a balance between enzymatic catalytic reactions and substrate transport dynamics. Salomi et al. [12] analyzed the transport and kinetic properties of polyphenol oxidase (PPO)-based bioelectrodes using rotating disk systems, emphasizing how rotation speed influences substrate diffusion and enzyme–substrate interactions. K. Lakshmi Narayanan et al. [13] developed a comprehensive mathematical model to quantitatively predict the performance of amperometric glucose biosensors, taking into account factors such as enzyme layer thickness, biosensor geometry, and diffusion mechanisms. Their work also broadened design considerations related to enzyme immobilization, substrate accessibility, and product transport efficiency. Arpit Goyal et al. [14] optimized electrochemical parameters, electrode materials, and reaction kinetics for a non-enzymatic amperometric biosensor designed for cholesterol detection, achieving improved sensitivity and stability. In addition, several related studies have

contributed to advancing modeling and analysis, including works by [28–37], all of which provide valuable insights into the development of efficient, robust, and application-oriented systems.

R. Shanthi et al. [15] further advanced the application of the Akbari-Ganji Method (AGM) by extending it to the analysis of pH-based potentiometric biosensors, focusing on the influence of ion-selective membrane characteristics and diffusion-reaction coupling on biosensor performance. R. Usha Rani et al. [16] investigated the relationship between diffusion length and reaction rate in biosensors, emphasizing how variations in catalyst shape and porosity impact catalytic activity within porous materials. Using a "What Went Wrong" analytical approach, Jeyabarathi et al. [17] applied the AGM to gain a deeper understanding of mass transfer dynamics in fixed-bed electrochemical reactors, improving current response and stability against operational disturbances. Raja et al. [21] performed a detailed mathematical analysis of polymeric coatings on microelectrodeskey components in biosensing systems-demonstrating how electrochemical kinetics and internal polymer resistance contribute to nonlinear current behavior. Swaminathan R. et al. [22] employed the Homotopy Perturbation Method (HPM) and Variational Iteration Method (VIM) to address nonlinear differential equations with variable coefficients arising in heat transfer, fluid flow, and spatially dependent chemical reaction studies. Additionally, Uma et al. [23] derived an analytical steady-state solution for concentrated hydrogen sulfide-methanol mixtures within biofilms, emphasizing the critical roles of microbial reaction kinetics and diffusion constraints in determining biofilm system behavior.

Nebiyal et al. [24] and Ranjani et al. [2,6] investigated nonlinear enzyme kinetics and multilayer diffusion effects in biosensors using the Akbari-Ganji Method. Reena et al. [4,25] modeled enzymatic putrescine biosensors integrating oxygen transport and biochemical response mechanisms. Other studies [19,26,27] advanced nonlinear modeling approaches for nanosensors, biofilters, and diagnostic biosensor performance prediction.

This study aims to solve various enzyme kinetic models using the Akbari–Ganji Method (AGM), a novel and efficient analytical technique for developing mathematical representations of steady-state biosensor systems. The structure of the paper is organized as follows: Section 2 presents the formulation of the proposed models; Section 3 provides their analytical solutions using the AGM; Section 4 includes numerical simulations performed in MATLAB; Section 5 discusses the obtained results; and Section 6 concludes the study with key findings and future perspectives.

### 2. Mathematical Formulation of the Problem

The analytical and biological behavior of biosensor systems is examined within membranes that geometrically represent substrate, product, and cosubstrate concentration profiles. Diffusion control becomes prominent, particularly when both electrodes are of identical size and enzymes are uniformly distributed across the active membrane. The one-dimensional diffusion process governing these systems is effectively described by Fick's second law. Diagnostic biosensor transducers typically incorporate oxygen electrodes, while the steady-state reaction-diffusion equation

in its loaded form is applied to characterize the dynamic behavior of such biosensor systems [18]. Consider the system of nonlinear second differential equations:

$$\frac{d^2S(\chi)}{d\chi^2} - \vartheta(S(\chi), C(\chi)) = 0, \tag{2.1}$$

$$\frac{1}{\lambda} \frac{d^2 P(\chi)}{d\chi^2} - \vartheta(S(\chi), C(\chi)) = 0, \tag{2.2}$$

$$\frac{1}{\mu\rho}\frac{d^2C(\chi)}{d\chi^2} - \vartheta(S(\chi), C(\chi)) = 0.$$
(2.3)

The non-dimensional coordinates, variables and parameters are:

$$\chi = \frac{\delta}{l}, S(\chi) = \frac{[S]}{K_S}, C(\chi) = \frac{[C]}{K_C}, P(\chi) = \frac{[P]}{K_P}, S_o = \frac{[S]}{K_S},$$
$$\lambda = \frac{D_S}{D_P}, \ \mu = \frac{D_S}{D_C}, \ \rho = \frac{K_S}{K_C} \text{ and } \phi = \frac{(\frac{V_m}{K_S})}{(\frac{l^2}{D_S})}.$$

The parameters for the diffusion coefficients of the substrate and co-substrate concentrations, and the product concentration are  $D_S$ ,  $D_C$ , and  $D_P$ , respectively. The reaction constant for conventional profiles C, S, P, and I for enzyme rate and spatial coordinate distance, respectively. The diagnoses of the biosensor system are in the transducer, reaction kinetics, and enzymatic kinetics. There are three categories of kinetics:  $D_S$ ,  $D_C$  and  $D_P$ . These biosensor systems employ the diagnostic feature of shared electrode geometry similarity and an even distribution of enzymes.

The first-order kinetics:

$$\frac{d^2S(\chi)}{d\chi^2} - \phi^2S(\chi) = 0, \tag{2.4}$$

$$\frac{1}{\lambda} \frac{d^2 P(\chi)}{d\chi^2} + \phi^2 S(\chi) = 0, \tag{2.5}$$

$$\frac{1}{\mu\rho} \frac{d^2 C(\chi)}{d\chi^2} - \phi^2 S(\chi) = 0. \tag{2.6}$$

The Michaelis-Menten kinetics:

$$\frac{d^2S(\chi)}{d\chi^2} - \frac{\phi^2S(\chi)}{1 + S(\chi)} = 0,$$
(2.7)

$$\frac{1}{\lambda} \frac{d^2 P(\chi)}{d\chi^2} + \frac{\phi^2 S(\chi)}{1 + S(\chi)} = 0, \tag{2.8}$$

$$\frac{1}{\mu\rho} \frac{d^2 C(\chi)}{d\chi^2} - \frac{\phi^2 S(\chi)}{1 + S(\chi)} = 0. \tag{2.9}$$

The Ping-Pong kinetics:

$$\frac{d^2S(\chi)}{d\chi^2} - \frac{\phi^2}{1 + \frac{1}{S(\chi)} + \frac{1}{C(\chi)}} = 0,$$
(2.10)

$$\frac{1}{\lambda} \frac{d^2 P(\chi)}{d\chi^2} + \frac{\phi^2}{1 + \frac{1}{S(\chi)} + \frac{1}{C(\chi)}} = 0,$$
(2.11)

$$\frac{1}{\mu\rho} \frac{d^2C(\chi)}{d\chi^2} - \frac{\phi^2}{1 + \frac{1}{S(\chi)} + \frac{1}{C(\chi)}} = 0.$$
 (2.12)

with the following boundary conditions to Equations (2.4)-(2.12):

$$\chi = 0, S(\chi) = s_0, P(\chi) = 0, C(\chi) = c_0,$$
 (2.13)

$$\chi = 1, \frac{dS(\chi)}{d\chi} = 0, P(\chi) = 0, C(\chi) = 0.$$
 (2.14)

In this formulation, l denotes the active membrane thickness,  $\phi$  represents the Thiele modulus,  $\lambda$  is the diffusion coefficient of the product,  $\mu$  corresponds to the diffusion coefficient of the cosubstrate, and  $\rho$  signifies the reaction rate constant between the substrate and co-substrate. The corresponding substrate, product, and co-substrate concentrations at the electrode surface are typically utilized to determine the biosensor's initial current, expressed as follows:

$$I_S = nFAD_S \left(\frac{dS(\chi)}{d\delta}\right)_{\delta=0},\tag{2.15}$$

$$I_{P} = nFAD_{P} \left( \frac{dS(\chi)}{d\delta} \right)_{\delta=0}, \tag{2.16}$$

$$I_{C} = nFAD_{C} \left( \frac{dS(\chi)}{d\delta} \right)_{\delta=0}.$$
 (2.17)

where n is the number of electrons taking part in electrochemical reaction, F is the Faraday's number, A is the electrode surface area  $[m^2]$ .

## 3. Approximate Analytical Solutions for the Steady-State Current and Concentrations Using the Akbari Ganji Method

The Akbari-Ganji Method (AGM) is a robust analytical technique used to obtain approximate solutions for nonlinear differential equations encountered in chemical and biochemical engineering. It is particularly effective for complex kinetic models where conventional analytical methods prove inadequate. By transforming nonlinear equations into a series of manageable linear subproblems, AGM facilitates the analysis of steady-state current and concentration distributions in reaction-diffusion systems. The selection of this method is guided by the nature and complexity of the problem under consideration [1].

In the case of first-order kinetics, the steady-state concentration profiles are obtained from equation (2.4) using the AGM, as given below:

$$S(\chi) = s_0 \cosh(m\chi) - \frac{\sinh(m) s_0 \sinh(m\chi)}{\cosh(m)}.$$
 (3.1)

where 
$$m = \phi$$
.

Using AGM, the solutions obtained from equation (2.5),

$$P(\chi) = \frac{-\lambda(\cosh(m\chi)\cosh(m) - \sinh(m)\sinh(m\chi) + (\chi - 1)\cosh(m) - \chi)s_0}{\cosh(m)}.$$
 (3.2)

where 
$$m = \phi$$
.

Using AGM, the solutions obtained from equation (2.6),

$$C(\chi) = \frac{\cosh(m\chi)\cosh(m) - \sinh(m)\sinh(m\chi) - (c_0)(\chi - 1)\cosh(m) - \chi}{\cosh(m)}.$$
 (3.3)

where 
$$m = \phi$$
.

For Michaelis-Menten kinetics using AGM, the solutions obtained from equation (2.7),

$$S(\chi) = s_0 \cosh(m\chi) - \frac{\sinh(m) s_0 \sinh(m\chi)}{\cosh(m)}.$$
 (3.4)

where 
$$m = \frac{\phi}{\sqrt{2}}$$
.

Using AGM, the solutions obtained from equation (2.8)

$$P(\chi) = \frac{-\lambda(\cosh(m\chi)\cosh(m) - \sinh(m)\sinh(m\chi) + (\chi - 1)\cosh(m) - \chi)s_0}{\cosh(m)}.$$
 (3.5)

where 
$$m = \frac{\phi}{\sqrt{2}}$$
.

Using AGM, the solutions obtained from equation (2.9),

$$C(\chi) = \frac{\cosh(m\chi)\cosh(m) - \sinh(m)\sinh(m\chi) - (c_0)(\chi - 1)\cosh(m) - \chi}{\cosh(m)}.$$
 (3.6)

where 
$$m = \frac{\phi}{\sqrt{2}}$$
.

For Ping Pong kinetics using AGM, the solutions obtained from equation (2.10),

$$S(\chi) = s_0 \cosh(m\chi) - \frac{\sinh(m) s_0 \sinh(m\chi)}{\cosh(m)}.$$
 (3.7)

where 
$$m = \frac{\sqrt{3} \phi}{3}$$
.

Using AGM, the solutions obtained from equation (2.11),

$$P(\chi) = \frac{-\lambda(\cosh(m\chi)\cosh(m) - \sinh(m)\sinh(m\chi) + (\chi - 1)\cosh(m) - \chi)s_0}{\cosh(m)}.$$
 (3.8)

where 
$$m = \frac{\sqrt{3} \phi}{3}$$
.

Using AGM, the solutions obtained from equation (2.12),

$$C(\chi) = \frac{\cosh(m\chi)\cosh(m) - \sinh(m)\sinh(m\chi) - (c_0)(\chi - 1)\cosh(m) - \chi}{\cosh(m)}.$$
 (3.9)

where 
$$m = \frac{\sqrt{3} \phi}{3}$$
.

Using AGM, the effectiveness factor for the equation (2.15),

$$S(\chi) = \frac{-(\cosh(m\chi)\cosh(m)-\sinh(m)\sinh(m\chi)+(-1)(\chi-1)\cosh(m)-\chi)}{\cosh(m)}.$$
 (3.10)

where 
$$m = \phi$$
.

Using AGM, the effectiveness factor for the equation (2.16),

$$S(\chi) = \frac{-(\cosh(m)\cosh(m\chi)s_0 - \sinh(m)\sinh(m\chi)s_0 - (s_0 + c_0)(\chi - 1)\cosh(m) - s_0 \chi)}{\cosh(m)}.$$
 (3.11)

where 
$$m = \frac{\phi}{\sqrt{2}}$$
.

Using AGM, the effectiveness factor for the equation (2.17),

$$S(\chi) = \frac{-(\cosh(m\chi)\cosh(m) - \sinh(m)\sinh(m\chi) - \chi)}{\cosh(m)}.$$
 (3.12)

where 
$$m = \frac{\sqrt{3} \phi}{3}$$
.

### 4. Numerical Simulation

The numerical simulation of the nonlinear reaction-diffusion system employed Equations (2.4)–(2.12) along with the boundary conditions in Equations (2.13) and (2.14) using MATLAB. These equations model the steady-state transport of substances across space while incorporating enzyme-mediated reactions through defined rate expressions. Simulations were conducted for three kinetic models: first-order, Michaelis-Menten, and Ping-Pong. By applying the steady-state assumption, the time-dependent terms were eliminated, reducing the system to a set of boundaryvalue problems for computational analysis. The specialized MATLAB script pdex4, developed for this analysis, is provided in the Appendix. The numerical and analytical results for each kinetic model are illustrated in the corresponding figures and tables. The numerical solutions closely agreed with the analytical predictions, exhibiting less than 1% maximum average relative error. The simulation outcomes confirm that the employed numerical scheme efficiently manages system nonlinearities with high precision. The results revealed clear steady-state concentration gradients, allowing for boundary current estimation via Fick's first law. Moreover, the selected kinetic model significantly influences the spatial enzyme distribution and the magnitude of the steady-state current, emphasizing the necessity of incorporating the full enzymatic mechanism in reactive diffusion modeling.

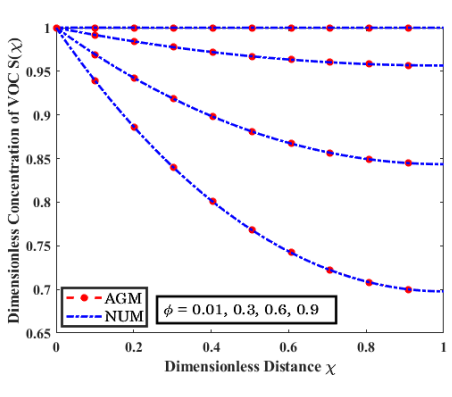
### 5. Result and Discussion

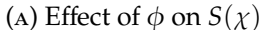
The graphical representations display the adjustments of dimensionless concentration  $S(\chi)$ ,  $P(\chi)$ , &  $C(\chi)$  concerning dimensionless distance  $\chi$  for different values of model parameters. The analytical results generated by the AGM method match exactly with numerical solutions (NUM), confirming the validity of the analytical techniques. Figure 1.(a), the substrate concentration  $S(\chi)$  shows a decreasing trend along the distance  $\chi$ , and this decrease becomes more pronounced as the parameter  $\phi$  increases. For lower values of  $\phi$ , the biosensor operates under kinetic-limited conditions, whereas for higher  $\phi$ , it transitions to a diffusion-limited regime. The concentration remains close to unity at  $\chi = 0$ , and decreases more steeply for larger  $\phi$ , indicating stronger diffusion effects. Figure 1.(b) presents the product concentration  $P(\chi)$  profiles for a fixed  $\phi = 0.3$  and varying  $\lambda$ . As  $\lambda$ , the ratio of diffusion coefficients, increases, the peak of  $P(\chi)$  becomes sharper and higher. It implies that increasing the diffusion ratio enhances the Thiele module and boosts product generation. Figure 1.(c), increasing  $\phi$  also increases the peak concentration of the product, further indicating that the product formation is sensitive to both enzyme concentration and diffusion characteristics. Figure 1.(d), the co-substrate concentration  $C(\chi)$  is plotted for varying  $\phi$ , keeping  $\rho = 1$  and  $\mu = 1$ . As  $\phi$  increases, the co-substrate concentration drops more rapidly along the domain, consistent with the transition from kinetic-limited to diffusion-limited behaviour. Figure 1.(e) examines the impact of increasing  $\mu$ , the ratio of diffusion coefficients. The co-substrate concentration decreases faster when  $\mu$  increases because high diffusion rates make co-substrate levels less available. Figure 1.(f) has an increased reaction rate ratio  $\rho$ , the co-substrate concentration shows a greater decline, which indicates that the reaction sink strength has a more substantial effect on concentration levels.

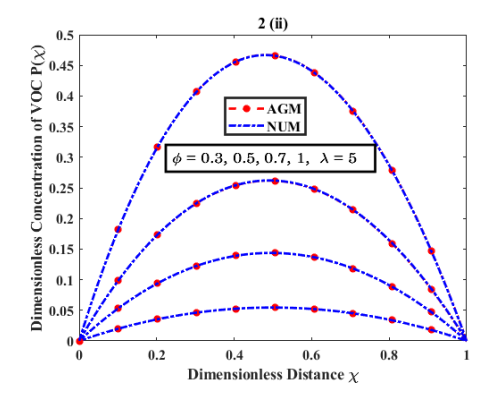
Figure 2.(a), the dimensionless concentration value of the substrate concentration  $S(\chi)$  decreases when the Thiele modulus value increases  $\phi$ . The adequate increment of  $\phi$  causes biosensor transitions from kinetic-limited to diffusion-limited control where reaction speed surpasses the diffusion rate. The concentration is highest near  $\chi = 0$  and gradually decreases toward  $\chi = 1$  When  $\phi$  equals 0.01, the system exhibits minimal diffusion resistance, which maintains the concentration level near unity across the entire domain. Figure 2.(b), the decrease of  $P(\chi)$  occurs at the enzyme zone, followed by a peak at the centre position as the diffusion coefficient ratio  $\lambda$  increases. The measurement shows that higher reactant transport enables greater product production. The biosensor encounters more favourable reaction conditions when  $\lambda$  increases, which results in amplified product accumulation within the middle zone. Figure 2.(c), the concentration profile of  $P(\chi)$  analysis occurs when the Thiele modulus  $\phi$  deepens. Producing less peak product remains a fact when the reaction rate rises since substrate availability decreases deep within the sensor. The locality of product formation at the entry zone emerges in reaction-dominant conditions because the substrate runs out. The dimensionless co-substrate concentration decreases more strongly along the distance  $\chi$ , according to Figure 2.(d), when  $\phi$  reaches higher values. The plot of  $C(\chi)$ shows a rapid decrease in its values as distance  $\chi$  increases. Reaction activity intensifies to deplete the co-substrate faster as a higher value of  $\phi$  is activated. A small value of  $\phi$  enables co-substrate diffusion to maintain higher levels throughout the sensor length. In Figure 2.(e), when the co-substrate diffusion ratio  $\mu$  increases, keeping  $\phi$  and  $\rho$  constant, the sensor maintains a substantial uniformity in co-substrate concentration distribution. The reaction effects become less pronounced at high diffusion ratios since enhanced transport improves substrate spread throughout the sensor volume. The levels of co-substrate sensor remain elevated throughout the length because a higher  $\mu$  generates a milder slope. Figure 2.(f) demonstrates the changes in the reaction rate constant ratio upon increasing values  $\rho$ . An increase in  $\rho$  value leads to a slight reduction of co-substrate concentration  $C(\chi)$ , particularly near the sensor centre and terminal regions. The reaction rate speeds up as enzyme-substrate affinity strength increases, which leads to further co-substrate depletion throughout the sensor and emphasizes kinetic restrictions.

Figure 3.(a) shows the dimensionless concentration of substrate  $S(\chi)$  starts at unity near  $\chi=0$ . The boundary represents a fresh supply because the value of  $\chi$  equals zero. The increasing value  $\phi$  sharpens the substrate concentration gradient, allowing diffusion effects to control the substrate consumption process. The distribution information for product  $P(\chi)$  appears in Figures 3.(b) and Figures 3.(c),  $P(\chi)$  for varying  $\lambda$  and  $\phi$ . The maximum product concentration occurs within the biosensor domain, and the concentration amount increases proportionately to elevated diffusion ratio values. The product concentration distribution within the biosensor increases as  $\lambda$  rises because improved reactant transport occurs. Likewise, for greater the sensor core generates additional product as the  $\phi$  parameter increases due to improved reaction efficiency. Figures 3.(d)–(f) shows the changing profile of co-substrate concentration  $C(\chi)$  under different conditions. As the Thiele modulus, rising value of  $\phi$  results in more prominent co-substrate exhaustion because the reaction becomes more intense. The distribution of co-substrate is more uniform throughout the length while having reduced concentration due to increased reaction consumption when  $\rho$  rises. The sensor shows linear variation of measurements, indicating steady and continuous change along its measurement region.

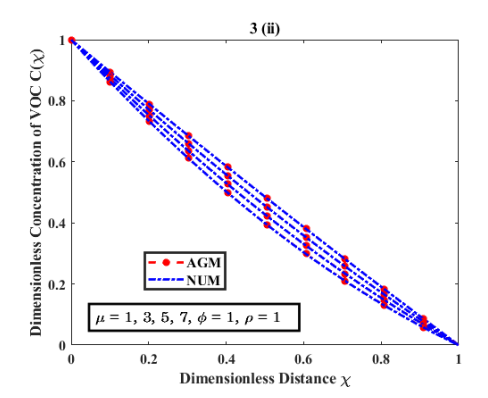
The variation of the dimensionless current with the Thiele module for different enzyme kinetic factors becomes visible in Figures 4.(a)–(c). Analysis of nonlinear biosensor models through the Akbari-Ganji method (AGM) and numerical solutions (NUM) demonstrated their compatible outcome, establishing AGM as an effective method in biosensor modeling. All scenarios show that the dimensionless current rises when the Thiele module value enlarges. The enhanced strength of the biosensor reaction-diffusion interaction results in a better current generation. A mild reaction regime is characterized by Figure 4.(a), which shows a smooth growth of the dimensionless current. Figure 4.(b) shows rapid growth because enhanced reaction rate constants or improved substrate-enzyme binding leads to better biosensor performance. The data in Figure 4.(c) exhibits a gradual current elevation about changes in the Thiele module at moderate kinetic conditions. The correct representation of nonlinear enzyme kinetics by the AGM solution demonstrates its capability to analyze diverse biosensor designs.



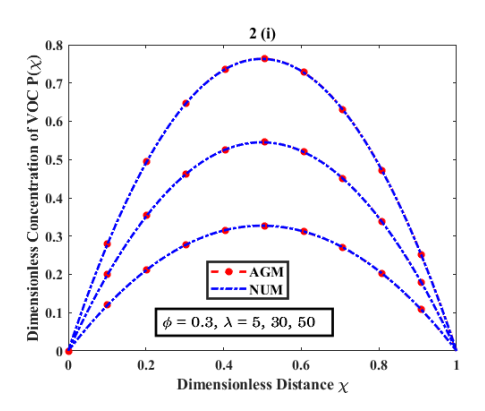




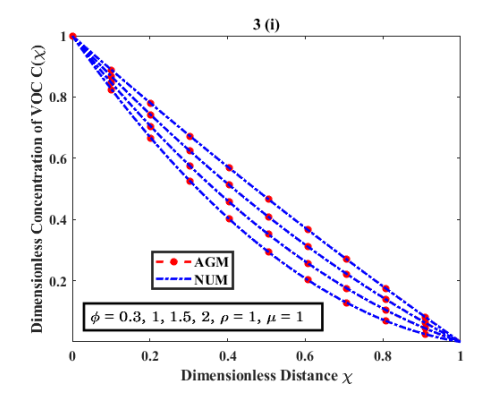
(c) Effect of  $\phi$  on  $P(\chi)$  with fixed  $\lambda$  and varying  $\phi$ 



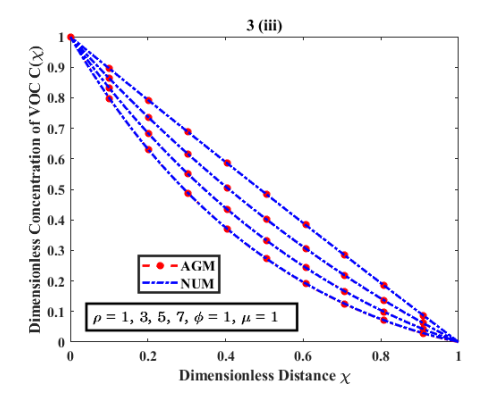
(E) Effect of  $\phi$  on  $C(\chi)$  with fixed  $\phi$ ,  $\rho$  and varying  $\mu$ 



(B) Effect of  $\phi$  on  $P(\chi)$  with fixed  $\phi$  and varying  $\lambda$ 

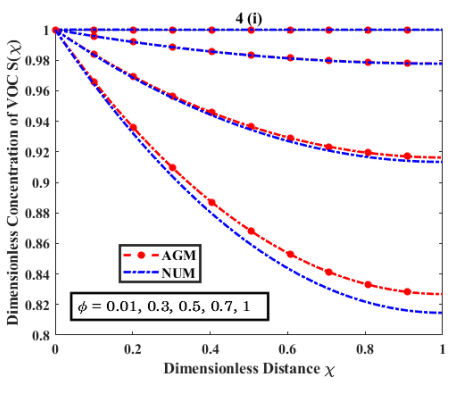


(D) Effect of  $\phi$  on  $C(\chi)$  with fixed  $\rho$ ,  $\mu$  and varying  $\phi$ 

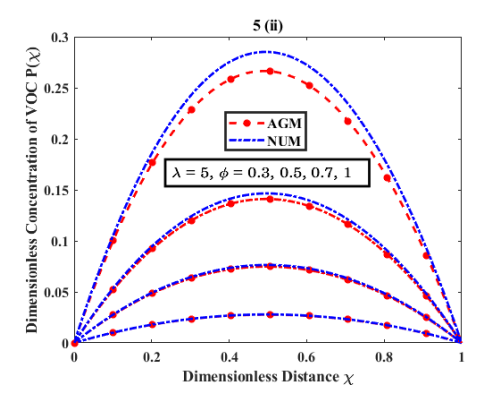


(F) Effect of  $\phi$  on  $C(\chi)$  with fixed  $\phi$  ,  $\mu$  and varying  $\rho$ 

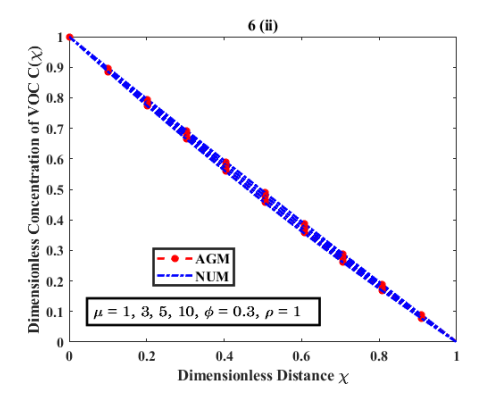
Figure 1. Graphical representation of the dimensionless concentrations of substrate  $S(\chi)$ , product  $P(\chi)$ , and co-substrate  $C(\chi)$  as functions of the dimensionless distance  $\chi$  for first-order kinetics, based on Equations (3.1), (3.2), and (3.3).



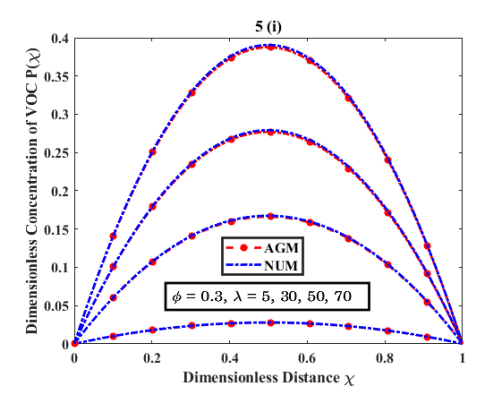
(a) Effect of  $\phi$  on  $S(\chi)$ 



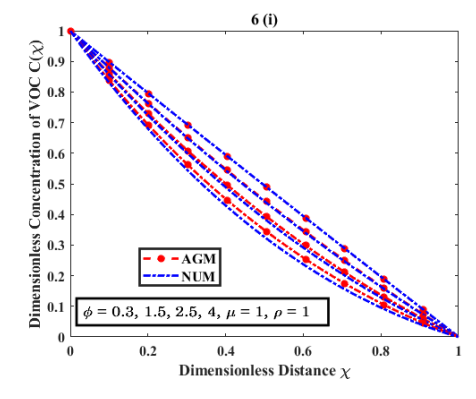
(c) Effect of  $\phi$  on  $P(\chi)$  with fixed  $\lambda$  and varying  $\phi$ 



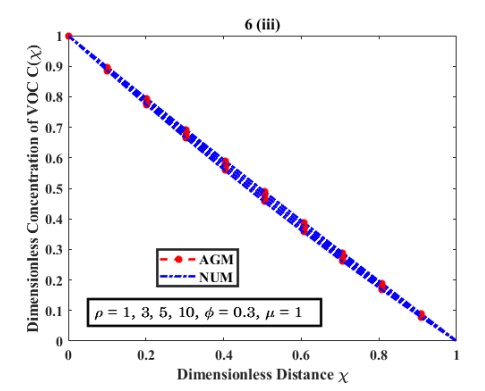
(E) Effect of  $\phi$  on  $C(\chi)$  with fixed  $\phi$ ,  $\rho$  and varying  $\mu$ 



(B) Effect of  $\phi$  on  $P(\chi)$  with fixed  $\phi$  and varying  $\lambda$ 

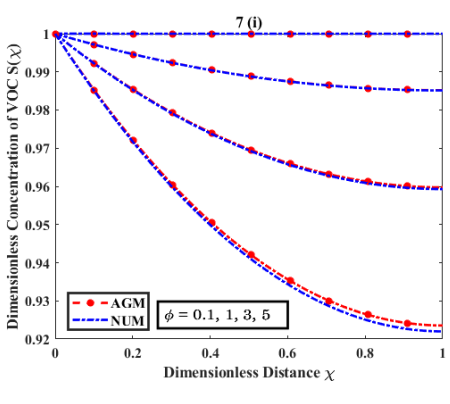


(D) Effect of  $\phi$  on  $C(\chi)$  with fixed  $\rho$ ,  $\mu$  and varying  $\phi$ 

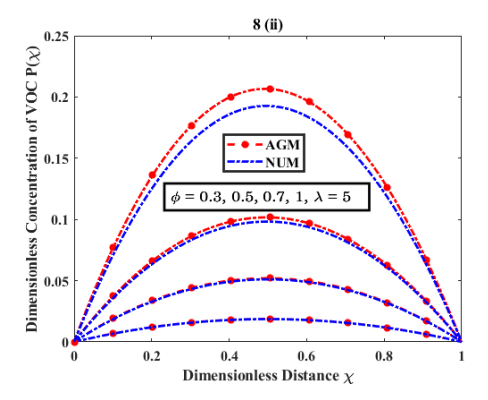


(F) Effect of  $\phi$  on  $C(\chi)$  with fixed  $\phi$  ,  $\mu$  and varying  $\rho$ 

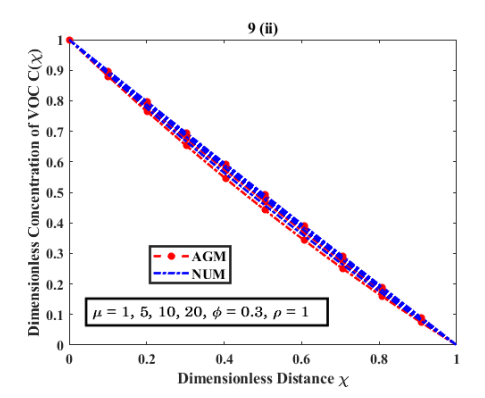
Figure 2. Graphical representation of the dimensionless concentrations of substrate  $S(\chi)$ , product  $P(\chi)$ , and co-substrate  $C(\chi)$  as functions of the dimensionless distance  $\chi$  for Michaelis–Menten kinetics, plotted from Equations (3.4), (3.5), and (3.6).



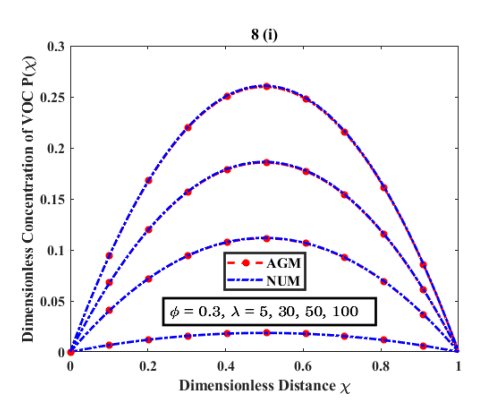
(a) Effect of  $\phi$  on  $S(\chi)$ 



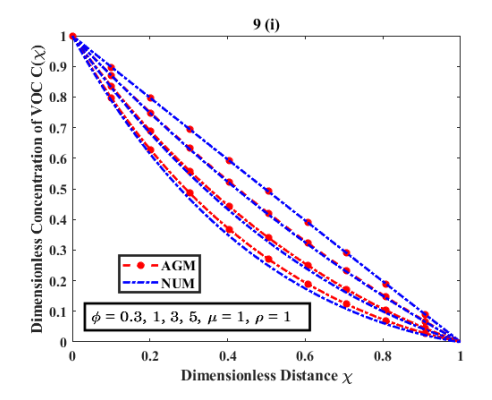
(c) Effect of  $\phi$  on  $P(\chi)$  with fixed  $\lambda$  and varying  $\phi$ 



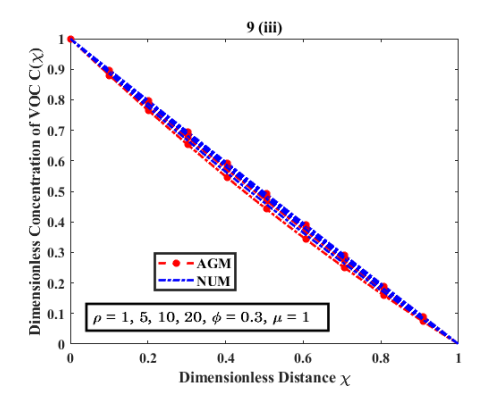
(E) Effect of  $\phi$  on  $C(\chi)$  with fixed  $\phi$ ,  $\rho$  and varying  $\mu$ 



(B) Effect of  $\phi$  on  $P(\chi)$  with fixed  $\phi$  and varying  $\lambda$ 



(D) Effect of  $\phi$  on  $C(\chi)$  with fixed  $\rho$ ,  $\mu$  and varying  $\phi$ 



(F) Effect of  $\phi$  on  $C(\chi)$  with fixed  $\phi$ ,  $\mu$  and varying  $\rho$ 

Figure 3. Graphical representation of the dimensionless concentrations of substrate  $S(\chi)$ , product  $P(\chi)$ , and co-substrate  $C(\chi)$  as functions of the dimensionless distance  $\chi$  for Ping–Pong kinetics, based on Equations (3.7), (3.8), and (3.9).

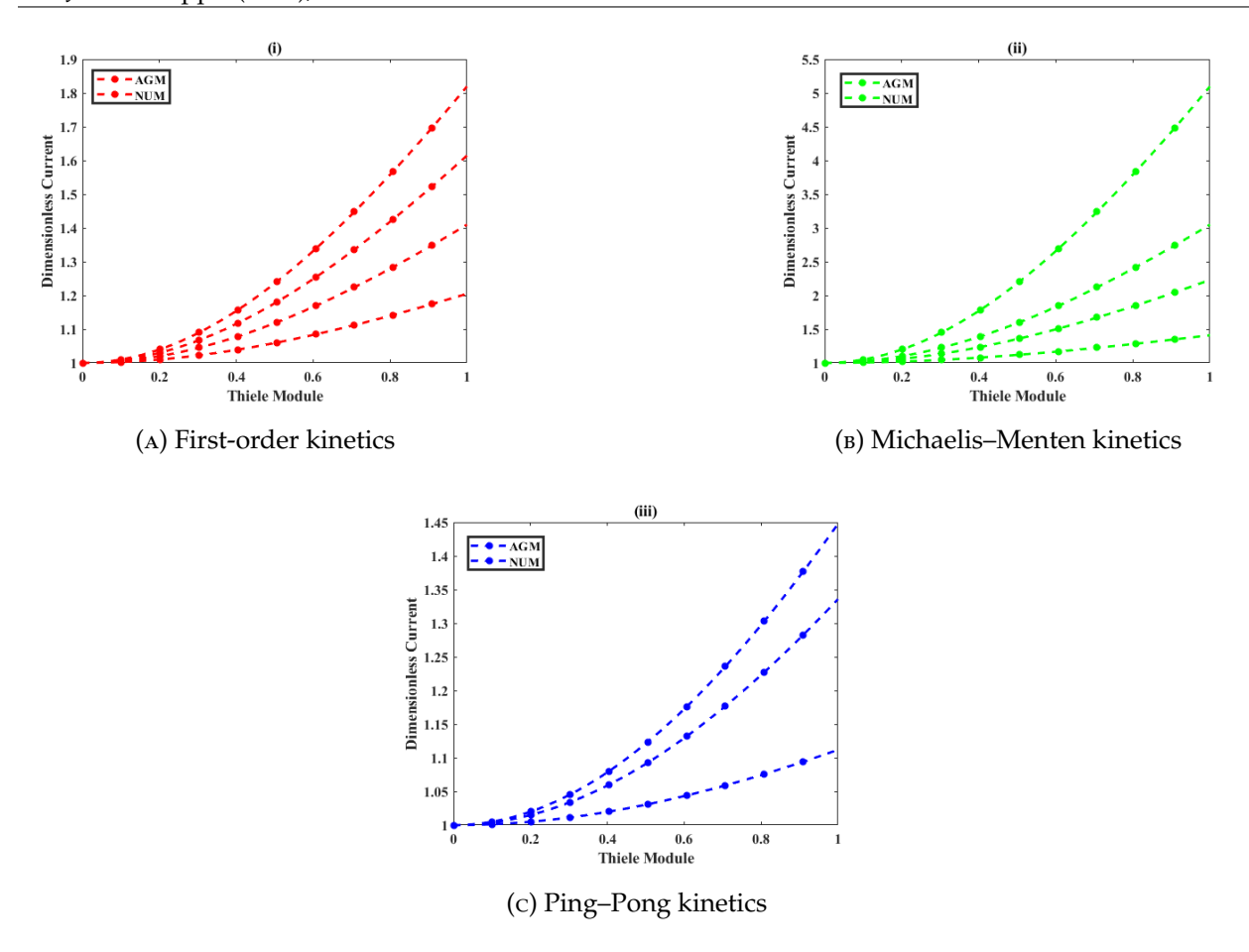


FIGURE 4. Graphical representation of the dimensionless current for the product versus the Thiele module for first-order, Michaelis–Menten, and Ping–Pong kinetics, based on Equations (3.10), (3.11), and (3.12).

	$\phi = 0.01$			$\phi = 0.3$			$\phi = 0.6$			$\phi = 0.9$		
Χ	AGM	NUM	Error%	AGM	NUM	Error%	AGM	NUM	Error%	AGM	NUM	Error%
χ	AGM	NUM	ERROR %	AGM	NUM	ERROR %	AGM	NUM	ERROR %	AGM	NUM	ERROR %
0	1	1	0	1	1	0	1	1	0	1	1	0
0.2	0.8856	0.8856	0	0.9421	0.9421	0	0.9841	0.9841	0	0.9999	0.9999	0
0.4	0.8005	0.8005	0	0.8980	0.8980	0	0.9719	0.9719	0	0.9999	0.9999	0
0.6	0.7420	0.7420	0	0.8672	0.8672	0	0.9633	0.9633	0	0.9999	0.9999	0
0.8	0.7081	0.7081	0	0.8491	0.8491	0	0.9582	0.9582	0	0.9999	0.9999	0
1	0.6977	0.6977	0	0.8435	0.8435	0	0.9566	0.9566	0	0.9999	0.9999	0
	Average Error % 0		0			0			0			0

Table 1. Comparison between the dimensionless concentrations  $S(\chi)$  from Equation (2.4) and numerical simulation results for first-order kinetics.

	$\phi = 0.01$			$\phi = 0.3$			$\phi = 0.6$			$\phi = 0.9$		
χ	AGM	NUM	Error%	AGM	NUM	Error%	AGM	NUM	Error%	AGM	NUM	Error%
0	1	1	0	1	1	0	1	1	0	1	1	0
0.2	0.9357	0.9318	0.4185	0.9683	0.9683	0	0.9918	0.9918	0	0.9999	0.9999	0
0.4	0.887	0.8796	0.8412	0.9457	0.9439	0.1906	0.9856	0.9856	0	0.9999	0.9999	0
0.6	0.8529	0.8428	1.1983	0.9291	0.9267	0.2589	0.9811	0.9811	0	0.9999	0.9999	0
0.8	0.833	0.8212	1.4369	0.9193	0.9165	0.3055	0.9785	0.9785	0	0.9999	0.9999	0
1	0.8268	0.8145	1.5101	0.9162	0.9134	0.3065	0.9777	0.9777	0	0.9999	0.9999	0
	Average Error%					0.1769			0			0

Table 2. Comparison between  $S(\chi)$  from Equation (2.7) and numerical results for Michaelis-Menten kinetics.

	$\phi=0.1$			$\phi = 1$			$\phi = 3$			$\phi = 5$			
χ	AGM	NUM	ERROR %	AGM	NUM	ERROR %	AGM	NUM	ERROR %	AGM	NUM	ERROR %	
0	1	1	0	1	1	0	1	1	0	1	1	0	
0.2	0.9714	0.9714	0	0.9851	0.9637	2.2206	0.9945	0.9945	0	0.9999	0.9999	0	
0.4	0.9504	0.9495	0.0947	0.9737	0.9355	4.0833	0.9904	0.9904	0	0.9999	0.9999	0	
0.6	0.9352	0.9339	0.1392	0.9655	0.9154	5.473	0.9874	0.9874	0	0.9999	0.9999	0	
0.8	0.9263	0.9248	0.1621	0.9612	0.9634	0.2283	0.9856	0.9856	0	0.9999	0.9999	0	
1	0.9235	0.9220	0.1626	0.9597	0.9996	3.9915	0.9851	0.9851	0	0.9999	0.9999	0	
	Average Error %		0.0931			1.2595			0			0	

Table 3. Comparison between the dimensionless concentrations  $S(\chi)$  from Equation (2.10) and numerical simulation results for Ping-Pong kinetics

### 6. Conclusion

This study developed an improved mathematical framework for analyzing steady-state concentration profiles and current responses in nonlinear reaction-diffusion systems governed by various enzyme kinetic mechanisms. The Akbari-Ganji Method (AGM) was employed as an efficient semi-analytical technique to derive approximate analytical solutions for enzyme reactions across different concentration regimes. Simulation results validated the accuracy and reliability of the AGM in capturing nonlinear system behavior through analytical expressions consistent with numerical outcomes. The findings revealed that spatial concentration distributions and current responses are highly influenced by the Thiele modulus, reaction rate constants, and diffusion coefficient ratios. Furthermore, the analysis identified critical transition points between distinct biosensor operating regimes, providing valuable insights for optimizing biosensor design and

performance. The AGM demonstrated a notable computational advantage over purely numerical methods due to its analytical formulation. Although the current model assumes steady-state conditions, uniform enzyme distribution, and ideal boundary constraints, which may limit full biological realism, it lays a strong theoretical foundation for future advancements. Future work will extend this approach to explore transient-state biosensor dynamics, non-uniform enzyme configurations, and multilayer biosensor architectures incorporating analytical and semi-analytical solutions.

**Acknowledgements:** The authors F. Hasan and N. Mlaiki would like to thank Prince Sultan University for paying the APC and for the support through the TAS research lab.

**Conflicts of Interest:** The authors declare that there are no conflicts of interest regarding the publication of this paper.

### References

- [1] L. Rajendran, R. Swaminathan, M.C. Devi, A Closer Look of Nonlinear Reaction-Diffusion Equations, Nova Science Publishers, 2020. https://doi.org/10.52305/RRSY7475.
- [2] K. Ranjani, R. Swaminathan, S. Karpagavalli, Mathematical Modelling of a Mono-Enzyme Dual Amperometric Biosensor for Enzyme-Catalyzed Reactions Using Homotopy Analysis and Akbari-Ganji Methods, Int. J. Electrochem. Sci. 18 (2023), 100220. https://doi.org/10.1016/j.ijoes.2023.100220.
- [3] R. Senthamarai, R. Jana Ranjani, Solution of Non-Steady-State Substrate Concentration in the Action of Biosensor Response at Mixed Enzyme Kinetics, J. Phys.: Conf. Ser. 1000 (2018), 012138. https://doi.org/10.1088/1742-6596/ 1000/1/012138.
- [4] A. Reena, S. Karpagavalli, R. Swaminathan, Theoretical Analysis and Steady-State Responses of the Multienzyme Amperometric Biosensor System for Nonlinear Reaction-Diffusion Equations, Int. J. Electrochem. Sci. 18 (2023), 100293. https://doi.org/10.1016/j.ijoes.2023.100293.
- [5] R. Joy Salomi, S. Vinolyn Sylvia, M. Abukhaled, M.E. Lyons, L. Rajendran, Theoretical Analysis of Transient Responses of Amperometric Biosensor Based on the Phenol–Polyphenol Oxidase Model, Int. J. Electrochem. Sci. 17 (2022), 22047. https://doi.org/10.20964/2022.04.42.
- [6] K. Ranjani, R. Swaminathan, S. Karpagavalli, A Theoretical Investigation of Steady-State Concentration Processes at a Carrier-Mediated Transport Model Using Akbari-Ganji and Differential Transform Methods, Partial. Differ. Equ. Appl. Math. 8 (2023), 100594. https://doi.org/10.1016/j.padiff.2023.100594.
- [7] K. Nirmala, B. Manimegalai, L. Rajendran, Steady-State Substrate and Product Concentrations for Non-Michaelis-Menten Kinetics in an Amperometric Biosensor-Hyperbolic Function and PadéApproximants Method, Int. J. Electrochem. Sci. 15 (2020), 5682–5697. https://doi.org/10.20964/2020.06.09.
- [8] R.U. Rani, N. Jha, L. Rajendran, A Theoretical and Computational Analysis of the Concentration of Substrate and Product in Enzyme-Based Electrochemical Biosensors: Akbari-Ganji's Method, J. Electroanal. Chem. 956 (2024), 118077. https://doi.org/10.1016/j.jelechem.2024.118077.
- [9] R. Swaminathan, M. Chitra Devi, L. Rajendran, K. Venugopal, Sensitivity and Resistance of Amperometric Biosensors in Substrate Inhibition Processes, J. Electroanal. Chem. 895 (2021), 115527. https://doi.org/10.1016/j.jelechem. 2021.115527.
- [10] S.M. Hashem Zadeh, M. Heidarshenas, M. Ghalambaz, A. Noghrehabadi, M. Saffari Pour, Numerical Modeling and Investigation of Amperometric Biosensors with Perforated Membranes, Sensors 20 (2020), 2910. https://doi. org/10.3390/s20102910.

- [11] S.V. Sylvia, R.J. Salomi, L. Rajendran, M. Lyons, Amperometric Biosensors and Coupled Enzyme Nonlinear Reactions Processes: A Complete Theoretical and Numerical Approach, Electrochimica Acta 415 (2022), 140236. https://doi.org/10.1016/j.electacta.2022.140236.
- [12] R. Joy Salomi, S. Vinolyn Sylvia, L. Rajendran, Transport and Kinetic Analysis of Amperometric Response Towards Ppo-Based Rotating Disk Bioelectrodes, J. Electroanal. Chem. 928 (2023), 117067. https://doi.org/10.1016/j.jelechem. 2022.117067.
- [13] K. Lakshmi Narayanan, J. Kavitha, R.U. Rani, M.E. Lyons, L. Rajendran, Mathematical Modelling of Amperometric Glucose Biosensor Based on Immobilized Enzymes: New Approach of Taylors Series Method, Int. J. Electrochem. Sci. 17 (2022), 221064. https://doi.org/10.20964/2022.10.47.
- [14] A. Goyal, P.K. Bairagi, N. Verma, Mathematical Modelling of a Non-enzymatic Amperometric Electrochemical Biosensor for Cholesterol, Electroanalysis 32 (2020), 1251–1262. https://doi.org/10.1002/elan.201900354.
- [15] R. Shanthi, M. Chitra Devi, M. Abukhaled, M.E. Lyons, L. Rajendran, Mathematical Modeling of Ph-Based Potentiometric Biosensor Using Akbari-Ganji Method, Int. J. Electrochem. Sci. 17 (2022), 220349. https://doi.org/10.20964/2022.03.48.
- [16] R.U. Rani, N. Jha, L. Rajendran, A Theoretical and Computational Analysis of the Concentration of Substrate and Product in Enzyme-Based Electrochemical Biosensors: Akbari-Ganji's Method, J. Electroanal. Chem. 956 (2024), 118077. https://doi.org/10.1016/j.jelechem.2024.118077.
- [17] P. Jeyabarathi, L. Rajendran, M.E.G. Lyons, M. Abukhaled, Theoretical Analysis of Mass Transfer Behavior in Fixed-Bed Electrochemical Reactors: Akbari-Ganji's Method, Electrochem 3 (2022), 699–712. https://doi.org/10. 3390/electrochem3040046.
- [18] P. Katzarova, V. Rangelova, S. Kuneva, Two Parameters Diagnostic of Biosensor Transducers, Biotechnol. Biotechnol. Equip. 20 (2006), 190–194. https://doi.org/10.1080/13102818.2006.10817331.
- [19] K.P.T. Preethi, V. Meena, R. Poovazhaki, Reliable Method for Steady-State Concentrations and Current Over the Diagnostic Biosensor Transducers, Am. J. Anal. Chem. 08 (2017), 493–513. https://doi.org/10.4236/ajac.2017.87036.
- [20] A. Reena, S. Karpagavalli, R. Swaminathan, Mathematical Analysis of Urea Amperometric Biosensor with Non-Competitive Inhibition for Non-Linear Reaction-Diffusion Equations with Michaelis-Menten Kinetics, Results Chem. 7 (2024), 101320. https://doi.org/10.1016/j.rechem.2024.101320.
- [21] A.D. Cathrine, R. Raja, R. Swaminathan, Mathematical Analysis of Nonlinear Differential Equations in Polymer Coated Microelectrodes, Contemp. Math. 5 (2024), 2569–2582. https://doi.org/10.37256/cm.5220244426.
- [22] R. Swaminathan, B. Manimegalai, K. Venugopal, L. Rajendran, Homotopy Perturbation Method and Variational Iteration Method for Solving the Nonlinear Equations with Variable Coefficients in Applied Sciences, AIP Conf. Proc. 2516 (2022), 130001. https://doi.org/10.1063/5.0108642.
- [23] A. Uma, R. Raja, R. Swaminathan, Analytical Solution of Concentrated Mixtures of Hydrogen Sulfide and Methanol in Steady State in Biofilm Model, Contemp. Math. 5 (2024), 2632–2645. https://doi.org/10.37256/cm.5320244394.
- [24] A. Nebiyal, R. Swaminathan, S. Karpagavalli, Reaction Kinetics of Amperometric Enzyme Electrode in Various Geometries Using the Akbari-Ganji Method, Int. J. Electrochem. Sci. 18 (2023), 100240. https://doi.org/10.1016/j. ijoes.2023.100240.
- [25] A. Reena, S. Karpagavalli, L. Rajendran, B. Manimegalai, R. Swaminathan, Theoretical Analysis of Putrescine Enzymatic Biosensor with Optical Oxygen Transducer in Sensitive Layer Using Akbari-Ganji Method, Int. J. Electrochem. Sci. 18 (2023), 100113. https://doi.org/10.1016/j.ijoes.2023.100113.
- [26] R. Saravanakumar, P. Pirabaharan, R. Swaminathan, Analysis of Nonlinear Vibrations of Double-Walled Carbon Nanotubes Using the Variational Iteration Method, Int. J. Res. 7 (2018), 342–348.
- [27] R.V. Raju, S. Karpagavalli, R. Swaminathan, Nonlinear Steady-State VOC and Oxygen Modeling in Biofiltration, Int. J. Anal. Appl. 22 (2024), 155. https://doi.org/10.28924/2291-8639-22-2024-155.

- [28] K. Dharmalingam, N. Jeeva, N. Alessa, Application of Chebyshev Polynomial-Exponential Method and Tamimi-Ansari Method in Dengue Transmission Dynamics: A Comparative Study, Int. J. Anal. Appl. 22 (2024), 219. https://doi.org/10.28924/2291-8639-22-2024-219.
- [29] S.E. Fadugba, M.C. Kekana, N. Jeeva, I. Ibrahim, Development and Implementation of Innovative Higher Order Inverse Polynomial Method for Tackling Physical Models in Epidemiology, J. Math. Comput. Sci. 36 (2025), 444–454. https://doi.org/10.22436/jmcs.036.04.07.
- [30] N. Jeeva, K.M. Dharmalingam, Numerical Analysis and Artificial Neural Networks for Solving Nonlinear Tuberculosis Model in SEITR Framework, Adv. Theory Simulations 8 (2025), 2401287. https://doi.org/10.1002/adts. 202401287.
- [31] K.M. Dharmalingam, N. Jeeva, N. Ali, R.K. Al-Hamido, S.E. Fadugba, et al. Mathematical Analysis of Zika Virus Transmission: Exploring Semi-Analytical Solutions and Effective Controls, Commun. Math. Biol. Neurosci. 2024 (2024), 112. https://doi.org/10.28919/cmbn/8719.
- [32] N. Jeeva, K.M. Dharmalingam, S.E. Fadugba, M.C. Kekana, A.A. Adeniji, Implementation of Laplace Adomian Decomposition and Differential Transform Methods for SARS-CoV-2 Model, J. Appl. Math. Inform. 42 (2024), 945–968. https://doi.org/10.14317/JAMI.2024.945.
- [33] N. Jeeva, K.M. Dharmalingam, Numerical Analysis of Skin Cancer Model Induced by Ultraviolet Radiation, Int. J. Biomath. 2024 (2024), 2450137. https://doi.org/10.1142/s1793524524501377.
- [34] N. Jeeva, K.M. Dharmalingam, Sensitivity Analysis and Semi-Analytical Solution for Analyzing the Dynamics of Coffee Berry Disease, Comput. Res. Model. 16 (2024), 731–753. https://doi.org/10.20537/2076-7633-2024-16-3-731-753.
- [35] S.E. Fadugba, N. Jeeva, A.E. Fdadugba, O. Faweya, A. Aloqaily, et al., Mathematical Modeling for the Analysis and Optimization of Nutrient Dynamics in Edible Mushrooms, Eur. J. Pure Appl. Math. 18 (2025), 7190. https://doi.org/10.29020/nybg.ejpam.v18i4.7190.
- [36] G. Rahman, C. Yildiz, M. Samraiz, S.S. Aiadi, N. Mlaiki, A Note on the Generalization of Minkowski's and Some Other Types of Integral Inequalities via Modified AB-Fractional Operator, J. Math. Comput. Sci. 40 (2025), 38–48. https://doi.org/10.22436/jmcs.040.01.03.
- [37] G. Mani, P. Ganesh, A. Aloqaily, A. Arulsamy, N. Mlaiki, Solving a Fractional Differential Equation via Extended Fuzzy Bipolar Metric Space, Int. J. Anal. Appl. 23 (2025), 265. https://doi.org/10.28924/2291-8639-23-2025-265.